Single-Phase Level Set Simulations for Unstructured Incompressible Flows

Clarence O. E. Burg*
Burg & Associates, Software Development for Education and Research, Starkville, MS, 39759

A robust unstructured nonlinear free surface simulation capability based on a single-phase level set has been developed and incorporated within a viscous, mixed-element incompressible Reynolds-averaged Navier-Stokes unstructured flow solver. This single-phase level set approach is applicable to simulations where the density ratio between the two fluids is sufficiently large enough so that the assumption that the less dense fluid has no impact on the free surface is reasonable. This assumption is valid for simulation of the free surface interface between water and air for viscous simulation of flow past surface ships. The single-phase level set assumes that the influence of the air on the interface can be ignored, and hence, the interface is wholly determined by the flow on the water side of the interface. In keeping with the level set paradigm, the flow is simulated on a fixed grid where the level set equation evolves to track the location of the interface, but only the waterside of the interface satisfies the incompressible RANS equations. On the air side, the velocity, pressure and turbulent quantities are extrapolated so as to be consistent with the water side of the interface. Several typical examples are shown, including the Wigley hullform, the Series 60 Cb=0.6 hullform and a naval destroyer DTMB Model 5415 hullform which has a transom stern.

Nomenclature

ϕ	=	level set parameter
$\vec{u}$	=	velocity vector
u_i	=	ith-velocity component
$\vec{x}$	=	coordinate location
P	=	pressure
L_∞, U_∞	=	Non-dimensional length and speed
ρ_∞, μ_∞	=	Non-dimensional pressure and viscosity
Fr	=	Froude number $\left(Fr = \frac{U_\infty}{\sqrt{gL_\infty}} \right)$
R_n	=	Reynolds number $\left(R_n = \frac{\rho_\infty U_\infty L_\infty}{\mu_\infty} \right)$
$\vec{F}, \vec{G}$	=	Convective or inviscid flux, diffusive or viscous flux
$\vec{Q}, Q_i, Q_L, Q_R$	=	Flow variables as a vector and as individual components at node or at faces

I. Introduction

FREE surface flows involving water and air are central to many different types of applications, including the flow through rivers and aqueducts, water elevations in lakes, oceans and other large bodies of water, which include

* President, 306 S. Jackson St., Starkville, MS, 39759, cburgburg1@yahoo.com, AIAA Member.

surface water, groundwater and rain water effects, and the flow around ships in motion and past structures such as oil platforms and buoys in the ocean. These flows have been studied for centuries, for irrigation of farmland, for storm water management and sewage disposal in large urban areas, and for transportation via ships. Free surface flows involve wave motion, as the flow is redirected by objects in the water or by changes in the topology of the region bounding the flow. Standing waves, cresting and breaking waves can be seen in a variety of situations, as trivial as the flow along street curbs to the waves that attract surfers to various locales around the world.

For naval vessels, the free surface introduces an additional form of drag, called wave drag, which is rarely seen in other fields, such as aircraft flight or in submarine simulations. This force affects the seaworthiness of the vessel as well as its maneuverability. In many cases, the free surface is principally governed by the Froude number which is related to the ratio of the kinetic energy with the potential energy associated with the wave elevations. For these cases, the viscous effects can be ignored when calculating the free surface, and scale models can be used to adequately predict the free surface. In addition, a myriad of approaches have been used to solve the inviscid free surface problem, most based on panel methods and potential flow theory. Several numerical codes have been developed to simulate the free surface about typical naval shapes, which run quickly on single processor machines. The performance of certain classes of ships can be adequately modeled using these inviscid methods, including planing ships that travel fast enough to rise up out of the water to a significant level, such as racing boats, ships that use hydrofoils to rise up out of the water, and slow speed container ships and large tankers which travel at 10-20 knots. For the hydrofoils and planning ships, a large amount of energy is expended in raising the ship out of the water so that the effects of viscous drag are of little relative importance. For slow speed ships, the viscous drag is reduced because of the slower speed. Additionally, design teams in the America's Cup yacht racing competition in several countries throughout the globe have expressed significant interest in inviscid and viscous free surface flows about their hullforms, including the effects of the wind/sail deflections and the subsequence changes in the orientation of the hull in the water and the water past the hull.

For naval ships, that travel at higher speed and that require a high level of efficiency and maneuverability, the viscous component of the flow is important. Typically, naval destroyers, such as the David Taylor Model Basin (DTMB) Model 5415 and the newer DDX series hulls, have transom sterns, which are truncated sterns. These sterns present severe challenges to free surface flow codes, because the transom is fully wetted for slower speeds, partially wetted for intermediate speeds and totally dry for higher speeds, so that building a single grid for the simulation at various speeds becomes problematic. Additionally, the wettedness of the transom appears to be influenced by the size of the ship, indicating that the Reynolds number has a significant influence on the shape of the free surface in the stern region. Since the Reynolds number plays a role in the shape of the free surface, it is also conjectured that the choice of turbulence model will play a role in these types of simulations.

Current research into the next generation of naval vessels will depend heavily on numerical viscous ship hydrodynamics, especially as naval designers investigate catamarans and trimarans, because of the increased seaworthiness and reduced wave signature afforded by these designs. Additionally, these ships will need to travel faster and carry heavier loads, so as to meet the challenges of the 21st century. Thus, minimization of viscous drag and wave drag will become increasingly important.

However, algorithms for robust and accurate simulation of the viscous free surface problem that are widely applicable to general hullform configurations, including rudders, shafts and rotating propellers and that can handle the physical complexity of cresting, breaking and re-entering waves, have been quite elusive. The incompressible Navier-Stokes equations presents some challenges for hyperbolic, finite volume methods, due to the need to alter the governing equations to fit within a hyperbolic framework. Boundary conditions along the viscous hull and for the free surface, especially at the intersection of the hull and free surface are problematic as well, especially for the pressure variable. The simulation of the viscous boundary layer, especially with the large variation in the velocity field within the boundary layer and the imposition of the no-slip viscous boundary condition, coupled with the changing shape of the free surface, which alters the computational domain, increases the difficulty of these simulations.

In order to meet these challenges, several different approaches have been investigated for robust and accurate simulation of the viscous flow around surface ships for naval hydrodynamic applications. The two primary paradigms are surface tracking and surface capturing. In surface tracking, the grid is moved to match the free surface while conforming to the grid, ignoring the flow on the air side of the free surface. Since this method simulates the free surface interface as a sharp interface, it typically is more accurate. However, surface tracking methods have limitations due to the need to be able to move the grid, which can be quite difficult for large amplitude wave motions. Several researchers[1-5] have implemented the surface tracking approach for structured grids, with good success for flows where the Froude number remains below 0.35 and where the viscous effects are not prevalent. An excellent example of this technology is the structured flow solver CFD-Ship-Iowa[2,3], which has been

validated for time-accurate roll-damping and maneuvering characteristics calculations. But only three researchers[6-8] have attempted this approach for unstructured grids, due to the difficulty of developing a robust grid movement algorithm, and one of these efforts has been limited to two-dimensional flows[8]. Each of these research teams is actively engaged in pursuing the more widely applicable surface capturing methodology.

The surface capturing paradigm solves the flow on a fixed grid and uses an auxiliary equation to specify the location of the free surface interface. This auxiliary equation, termed the level set equation, is defined below as

$$\frac{\partial \phi}{\partial t} + \vec{u} \cdot \nabla \phi = 0 \tag{1}$$

Where $\vec{u}$ is the velocity vector and ϕ is the level set function, which is interpreted in various manners based on the type of surface capturing algorithm. For the volume-of-fluid approach, the level set ranges from 0 to 1 and specifies the percentage of the volume which is occupied by the two fluids, with the interface typically being located at 0.5. For the single-phase approach, the level set is typically a signed distance function from the interface, so that 0 defines the interface, or

$$\phi(\vec{x}) = \begin{cases} < 0 & \text{if } \vec{x} \text{ is in water} \\ 0 & \text{if } \vec{x} \text{ is at free surface} \\ > 0 & \text{if } \vec{x} \text{ is in air} \end{cases} \tag{2}$$

Since the grid does not move, the simulations are typically much more robust and more widely applicable. In the volume-of-fluid approach[9,10], the level set function is used to specify the ratio of the control volume to be considered as fluid A and as fluid B. Thus, the density and viscosity are blended values for cells near the air/water interface, and this interface is thereby blurred over a small number of cells. Interface sharpening is used to rebuild the interface, but this blurring can degrade the accuracy of the simulation. The volume-of-fluid approach is an older technology and has been implemented within some commercial software codes, such as CFX[11] and Comet[12], both of which rely on unstructured simulation methodologies.

The other class of level set simulations is the single-phase level set approach, where the air side of the simulation is ignored. The level set defines a distance to the interface, rather than the ratio of fluid densities. The solution variables are extrapolated from the water side into the air so that the interface evolves naturally. Hence, the interface between the water and air is modeled as a crisp interface, which more readily reflects the physical world. In addition, because the interface is not smeared, it can be captured within one cell, so that the grid resolution near the interface does not need to be significantly different from the rest of the grid. This surface capturing methodology has been successfully implemented within the structured flow solver developed by researchers at Insean in Italy[13].

In this paper, the single-phase level set approach is implemented within the viscous unstructured flow solver U^{2}NCLE, developed by researchers within the Computational Simulation and Design Center at Mississippi State University. On the water side of the interface, the typical finite volume methodology is used to discretize and solver the RANS equations. The level set equation is solved near the interface and then is reinitialized using the Laplacian $\nabla^2 \phi = 0$ to mimic the distance function behavior of the level set parameter. The velocity is extrapolated into the air side so that $\nabla u_i \cdot \nabla \phi = 0$ for each velocity component, and the pressure is set to $P = \frac{(y - \phi)}{Fr^2}$ which imposes the proper pressure distribution along the free surface interface where $\phi = 0$ and is consistent with the inflow boundary where $\phi = y$ and $P = 0$.

The governing equations and discretization methods involved with the RANS solver and the level set implementation are presented in the next section. Several examples are presented in the following section, including several grid refinement studies for inviscid simulations and the results of some intriguing possibilities for this methodology. Conclusions and ideas for future improvements to this methodology are in the final section.

II. Governing Equations and Numerical Approach

A. Governing Equations for Reynolds-averaged Navier Stokes Equations

The incompressible Reynolds-averaged Navier-Stokes (RANS) equations consist of an equation for the conservation of mass and three equations for the conservation of momentum. After non-dimensionalizing, these equations can be written as

$$\begin{aligned} \nabla \cdot \vec{u} &= 0 \\ u_t + uu_x + vu_y + wu_z &= \\ &\quad -P_x + \frac{(\mu + \mu_t)}{R_n}\nabla^2 u \\ v_t + uv_x + vv_y + wv_z &= \\ &\quad -P_y + \frac{(\mu + \mu_t)}{R_n}\nabla^2 v \\ w_t + uw_x + vw_y + ww_z &= \\ &\quad -P_z + \frac{(\mu + \mu_t)}{R_n}\nabla^2 w \end{aligned} \tag{3}$$

where $\vec{u} = (u, v, w)$ is the velocity vector in the x, y and z coordinate directions, P is the dynamic pressure, μ and μ_t are the molecular and turbulent viscosity, and R_n is the Reynolds number.

In order to apply standard finite volume methods to this set of equations, Chorin's concept of artificial compressibility[14] is used to convert the continuity equation into time-marching form. The use of artificial compressibility permits the experience gained in the numerical solution of hyperbolic compressible-flow problems to be exploited in the solution of incompressible-flow problems[15-17]. Using artificial compressibility, the governing equations can be written in integral form as:

$$\frac{\partial}{\partial t}\int_{\Omega} Q\, dV + \int_{\partial\Omega} \vec{F}\cdot\hat{n}\, dA = \frac{1}{R_n}\int_{\partial\Omega} \vec{G}\cdot\hat{n}\, dA \tag{4}$$

where

$$Q = \begin{bmatrix} P \\ u \\ v \\ w \end{bmatrix}, \quad \vec{F}\cdot\hat{n} = \begin{bmatrix} \beta\Theta \\ u\Theta + \hat{n}_x P \\ v\Theta + \hat{n}_y P \\ w\Theta + \hat{n}_z P \end{bmatrix} \tag{5}$$

$$\vec{G}\cdot\hat{n} = \begin{bmatrix} 0 \\ \hat{n}_x\tau_{xx} + \hat{n}_y\tau_{xy} + \hat{n}_z\tau_{xz} \\ \hat{n}_x\tau_{yx} + \hat{n}_y\tau_{yy} + \hat{n}_z\tau_{yz} \\ \hat{n}_x\tau_{zx} + \hat{n}_y\tau_{zy} + \hat{n}_z\tau_{zz} \end{bmatrix} \tag{6}$$

where β, typically set to 15, is the artificial compressibility parameter and Θ is the velocity dotted into the surface normal and is defined as:

$$\Theta = \hat{n}_x u + \hat{n}_y v + \hat{n}_z w \tag{7}$$

The variables in the preceding equations are non-dimensionalized, using a characteristic length L_∞, such as the length of the ship, and free stream values of velocity U_∞, density ρ_∞, and viscosity μ_∞. Thus, the Reynolds number is defined as:

$$R_n = \frac{\rho_\infty U_\infty L}{\mu_\infty} \tag{8}$$

Pressure is normalized with:

$$P = \frac{P^* - P_\infty}{\rho_\infty U_\infty^2} \tag{9}$$

where P^* is the local dimensional pressure and P_∞ is the ambient pressure. The viscous stresses are:

$$\tau_{ij} = (\mu + \mu_t)\left(\frac{\partial u_i}{\partial x_j} + \frac{\partial u_j}{\partial x_i}\right) \tag{10}$$

where $u_1 = u$, $u_2 = v$, $u_3 = w$, $x_1 = x$, $x_2 = y$, $x_3 = z$. Several turbulence models are available within the unstructured flow solver, including the two-equation $k-\varepsilon$, $k-\sigma$ and $q-\sigma$ turbulence models. However, the single equation Spalart-Allmaras turbulence model[18] is used for the viscous simulations dealing with the single-phase surface capturing methodology. The results presented herein do not involve the viscous boundary layer, so the influence of the turbulence modeling is negligible for the current simulations.

B. Unstructured Flow Solver U^{2}NCLE.

The U^{2}NCLE code is a viscous unstructured flow solver of the incompressible and compressible forms of the Reynolds-averaged Navier-Stokes equations using the flux differencing finite volume methodology using Roe-averaged variables[19] to evaluate the convective fluxes and the directional derivative method to approximate the gradient at the faces of the control volumes in order to evaluate the diffusive fluxes. This methodology has been extensively validated on a variety of geometries of interest to the naval architect, including isolated appendages (rudders and propellers), bare hull, and fully-appended submarines and surface ships, including those with operating rotating propellers [20-22]. A more detailed description of the solution methodology within the U^{2}NCLE code are available[23,24]. The unstructured grids are mixed element grids that are built using the Advancing Front/Local-Reconnection algorithm developed by Marcum, et al[25,26]. These grids consist of highly stretched anisotropic prismatic elements within the boundary that transition through the use of pyramids into a tetrahedral region away from the viscous surface.

Starting with equation (2), the convective fluxes $\vec{F}$ are discretized at the faces of the control volume by evaluating the flux at the center of the faces, or

$$\int \vec{F} \cdot \hat{n}\, dA \approx \sum_{i \varepsilon \kappa(0)} \vec{F}_{0i} \cdot \hat{n}_{0i} \tag{11}$$

where the summation is performed around all the surrounding nodes (e.g. nodes 1 through 7 in Figure 1), and $\hat{n}$ is the outward-pointing unit normal to the control volume Ω, and A is the surface area of the control volumes. This discretization methodology ensures that conservation of mass and momentum. Both the inviscid and viscous fluxes are discretized by evaluation at the surfaces of the control volume. Hence, the flow variables and their gradients must be evaluated at these faces. Once the flow variables are evaluated, then the convective flux is evaluated using

the upwinded flux differencing method, using Roe-averaged variables. The diffusive or viscous fluxes are evaluated directly from the gradients.

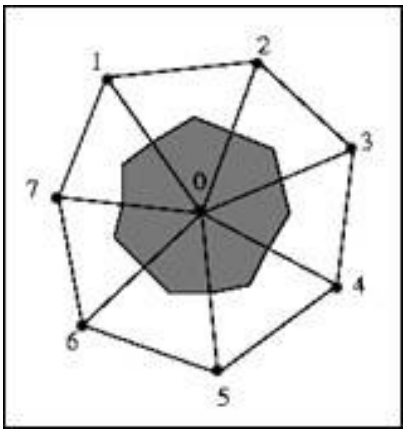

Figure 1. Typical dual-control volume for a cell-centered finite volume approach.

The newly developed Unstructured MUSCL (U-MUSCL) approach[27] is used to extrapolate the flow variables to the face of the control volume, by using the values at the nodes on either side of the face and the appropriate gradient. This formula is third-order accurate for this part of the discretization and can be expressed as

$$Q_L(\chi) = Q_i + \frac{\chi}{2}(Q_j - Q_i) + (1-\chi)\nabla Q_i \bullet \hat{r}_{ij} \tag{12}$$

where χ is the U-MUSCL parameter, set to 0.5, Q_i and Q_j are the flow variables at the nodes on either side of the face, ∇Q_i is the gradient of Q at node i, calculated via least-squares, and $\hat{r}_{ij}$ is the vector between nodes i and j.

The viscous fluxes require that the gradient of the velocities are approximated at the faces of the control volumes, since these fluxes consistent of the derivatives of the velocity dotted into the face normals. Gradient information is available at the nodes, and a simple average of these gradients could be used at the face. Similarly, since the face normal and the edge vector between the nodes are roughly in the same direction, the difference in the nodal values can be used to approximate the normal derivative along each edge. These two approximations to the derivative are used in the following formula to estimate the gradient at the face of the control volume, which is attributed to Hyams and Marcum[24]

$$\nabla Q_f = \frac{\nabla Q_i + \nabla Q_j}{2} + \left[\frac{Q_j - Q_i}{\left\| \hat{r}_{ij} \right\|} - \frac{\nabla Q_i + \nabla Q_j}{2} \bullet \frac{\hat{r}_{ij}}{\left\| \hat{r}_{ij} \right\|} \right] \hat{r}_{ij} \tag{13}$$

Once the temporal component, the inviscid and viscous components are discretized, a large, sparse system of nonlinear equations results. This system is solved using Discretized Newton Relaxation[28,29], with multiple Gauss-Seidel subiterations.

C. Single-Phase Level Set Governing Equations and Discretization Methods

The U^{2}NCLE code has been modified to solve the free surface using the single-phase level set methodology. In this methodology, the incompressible RANS equations are solved in the water side without any modifications to the proven incompressible flow solver. On the air side and near the interface, other methods are used to determine the pressure and the velocity. The velocities are propagated into the air from below the interface so that the velocity is smooth across the interface, while the pressures are set on the air side based on the value of the level set parameter. The level set equation is solved in a small region about the interface and then is reinitialized outside of this band. The region and the solution methodology are shown in Figure 2.

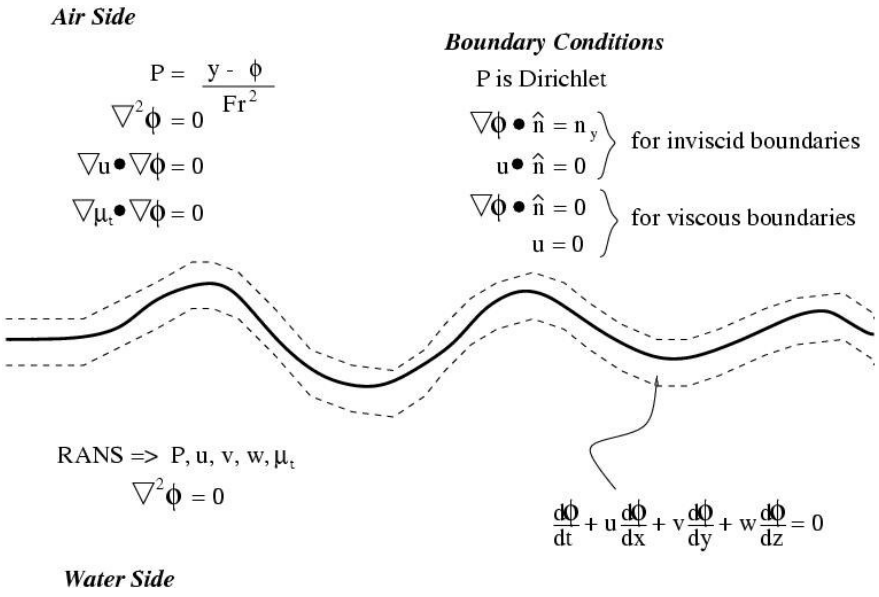

Figure 2. Regions within the computational domain, showing the equations solved in each region.

The level set equation is solved using the finite volume method by converting it into appropriate hyperbolic form, or

$$0 = \frac{\partial \phi}{\partial t} + \vec{u} \cdot \nabla \phi = \frac{\partial \phi}{\partial t} + \nabla(\vec{u}\phi) - \phi \nabla \cdot \vec{u} \tag{14}$$

For the water side of the equations, the flow is incompressible, or $\nabla \cdot \vec{u} = 0$, but the manner by which the velocities are extrapolated into the air side does not guarantee incompressibility, so this term is left in the equation. Applying the finite volume method, integrating over the control volume, the discretized equation is

$$\int_{\Omega} \frac{\partial \phi}{\partial t} + \nabla(\vec{u}\phi) - \phi \nabla \cdot \vec{u} \approx \int_{\Omega} \frac{\partial \phi}{\partial t} + \int_{\partial\Omega} \phi \vec{u} \cdot \hat{n}\, dA - \phi \int_{\partial\Omega} \vec{u} \cdot \hat{n} = 0 \tag{15}$$

There is an approximation within the last term of the expression, since ϕ is not constant, but this term plays only a minor role since it is the term associated with the level of compressibility in the flow. Boundary conditions for the hull and at the outer boundaries are well defined, using the appropriate values of $\vec{u} \cdot \hat{n}$. The level set equation is solved for three nodes on either side of the interface, so away from the interface, the level set parameter is determined by solving the Laplacian, or $\nabla^2 \phi = 0$, which can be discretized via the finite volume method as

$$\int_{\Omega} \nabla^2 \phi \, d\Omega = \int_{\partial\Omega} \nabla \phi \cdot \hat{n} = 0 \tag{16}$$

with the boundary condition of $\nabla \phi \cdot \hat{n} = n_y$ along the hull, which implies that the free surface is flat as it approaches the hull. At the outer boundary, a Dirichlet boundary condition is used, with $\phi = y$ which assumes that there is no free surface distortion at the outer boundary. If the outer boundary is sufficiently far away and if the scheme is sufficiently diffusive, then this assumption is valid.

The pressure and velocity are solved on the water side of the interface using the flux-differencing finite volume method described in the previous section. For the edges that intersect the free surface, the pressure that would be calculated via the extrapolation to the control volume face is replaced by the hydrostatic pressure, defined by

$$P = \frac{\left(y_{\text{int}\,erface} - \phi_{\text{int}\,erface}\right)}{Fr^2} \tag{17}$$

where the interface values are the average of the nodal values at either end of the edge. DiMascio uses a different methodology to calculate the hydrostatic pressure at the control volume face, but his methodology assumes a structured grid.

For the nodes on the air side of the interface, the velocity is determined by extrapolating the velocity components so that the velocity field is roughly tangent to the free surface interface. Thus, each component is determined by solving

$$\nabla u_i \cdot \nabla \phi = 0 \tag{18}$$

using the finite volume formulation, which becomes

$$0 = \int_\Omega \nabla u_i \cdot \nabla \phi = \int_\Omega \nabla \cdot \left(u_i \nabla \phi\right) - u_i \nabla^2 \phi \approx \int_{\partial\Omega} u_i \nabla \phi \cdot \hat{n}\, dS - u_i \int_{\partial\Omega} \nabla \phi \cdot \hat{n}\, dS \tag{19}$$

The boundary condition for the free surface is $\nabla \phi \cdot \hat{n} = n_y$ on the hull and on the outer boundaries.

III. Numerical Examples

Several numerical examples are presented herein showing the wide applicability of the single-phase level set methodology. Results for the parabolic Wigley hullform and the more realistic Series 60 Cb=0.6 hullform are presented along with a grid refinement study for both hulls. The free surface around a typical naval destroyer, the David Taylor Model Basin (DTMB) Model 5415 hullform is also shown. Additionally, the free surface results for a typical America's Cup geometry and for a water cannon are presented, showing the range of applications of this methodology.

A. Wigley Hull

The Wigley hullform is a mathematically defined parabolic shape, as defined by

$$z(x, y) = \frac{B}{2}\left(1 - 4x^2\right)\left(1 - \left(\frac{y}{D}\right)^2\right) \tag{20}$$

where B is the maximum thickness of the hull and D is the draft of the hull and are set to 0.1 and 0.0625 respectively. This hullform has been studied at a variety of speeds in numerous experimental and numerical simulations, due to its geometric simplicity[30]. The geometry creates a strong bow wave and a stern wave, which are both typical of ships flowing in water. The shape of the free surface along the hull and the associated wave drag has been measured experimentally, and this geometry is a typical first geometry for free surface simulations pertaining to ship hydrodynamics.

Thus, the Wigley hull was the first hullform on which the unstructured implementation of the single-phase level set method was applied. A series of unstructured, tetrahedral grids were generated by successively increasing the point spacing within the CAD geometry, by using a ratio of $\sqrt[3]{2}$. Thus, for the volume grid, the number of tetrahedral and the number of nodes should decrease by roughly a factor of 2 from one grid level to the next. The fine grid consisted of 2,079,188 nodes, while the medium grid had 1,093,330 nodes and the coarse grid had 583,930, demonstrating an appropriate reduction in the number of nodes. Only one side of the hull and domain is gridded, taking advantage of its symmetry. The free surface profiles along the hull for a Froude number of 0.289 are shown in Figure 3 for the three grids. The bow wave reaches the highest for the fine grid and dips down the furthest in the troughs along the hull, apparently converging towards the experimental data.

The single-phase level set methodology is clearly diffusive away from the hull, as is shown in Figures 4 and 5, with the bow and stern waves dissipating approximately one ship length behind their origin. Figure 4 shows a three-dimensional view of the free surface, with the flow coming from left to right. Figure 5 shows the wave elevations from above. By placing more points near these wave patterns, these waves can be propagated further.

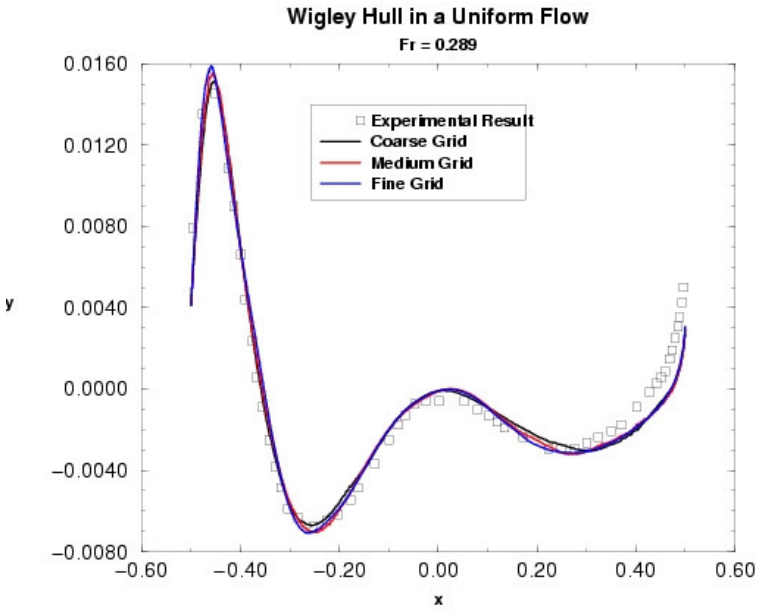

Figure 3. Water elevation along Wigley hull.

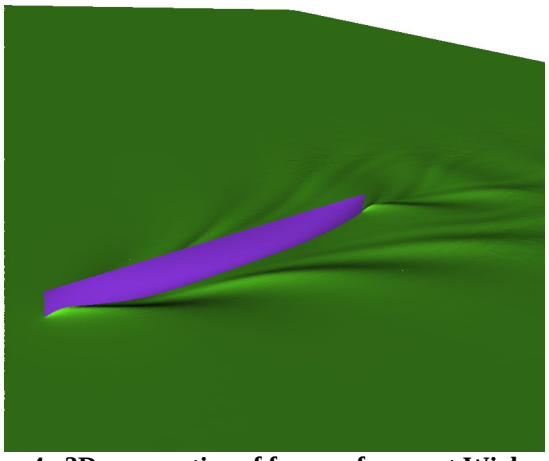

Figure 4. 3D perspective of free surface past Wigley hull.

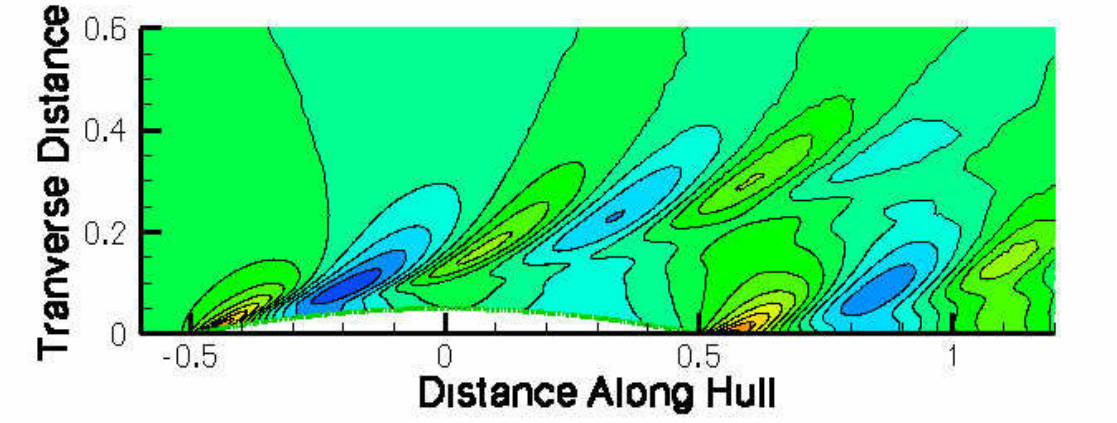

Figure 5. Overview of wave elevations past Wigley hull, showing that the free surface is maintained to approximately one hull length downstream of origin.

B. Series 60 Cb=0.6 hullform

The Series 60 Cb=0.6 hullform is another classic hullform for numerical and experimental simulations. Its geometry is more characteristic of actual ships and includes a region in the stern for possible rudder and propeller, but the bow is more characteristic of the Wigley hull. Much experimental data is available for this geometry, including velocity and wave elevation cuts at various locations through the flow field.

The inviscid flow condition results in a Froude number of 0.316 which is higher than for the Wigley hullform. Three grids were built, using the same refinement ratio as for the Wigley hull, resulting in a fine grid with 1,719,241 nodes, a medium grid with 958,502 nodes and a coarse grid with 550,421. The number of nodes is slightly more than half for each successively coarsened grid, due to the increased geometric complexity of the hullform. Additionally, both sides of the geometry were gridded for this geometry, so that the relative number of points is smaller for this simulation than for the Wigley hull. The results for the fine grid are presented in Figure 6 and show that the solution is tending towards the same extremes in the peaks and troughs as the experimental measurements. The difference in the free surface from the coarse grid to the fine grid is hardly noticeable, indicating that the grid refinement is adequate for these inviscid simulations.

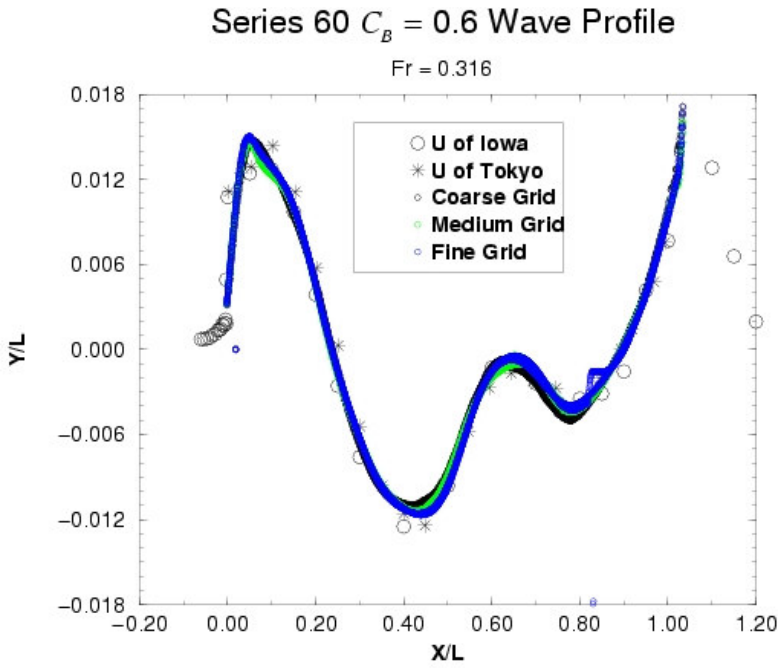

Figure 6. Water elevation along Series 60 hullform

In Figures 7 and 8, a three-dimensional representation of the free surface and an overview of the free surface elevations from above are shown. Due to the coarseness of the grid away from the ship, the free surface dissipates rapidly, with bow and stern waves disappearing well before one ship length from their origin. However, this coarsening does not appear to affect the accuracy of the free surface along the hull.

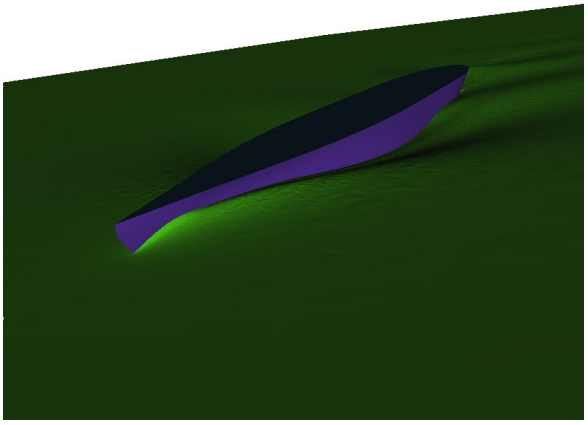

Figure 7. 3D perspective of free surface past Series 60 hullform.

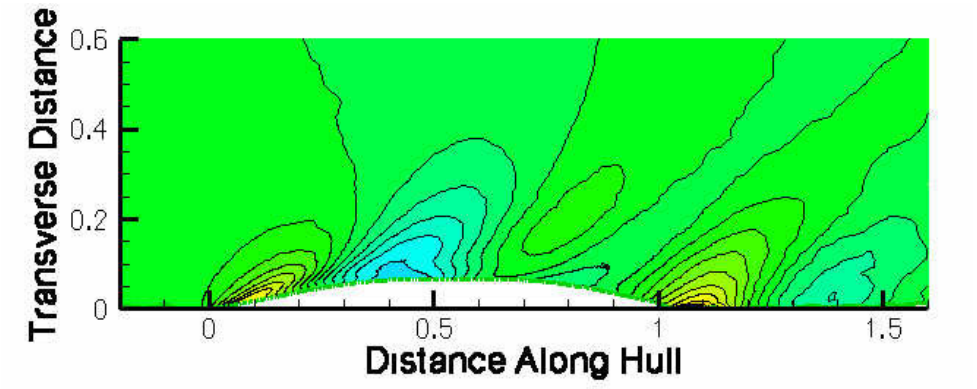

Figure 8. Overview of wave elevations past Series 60 hullform.

In Figure 9, the surface grid for the Series 60 Cb=0.6 hullform is shown along with the location of the free surface as predicted by the single-phase level set approach. As is seen in the figure, the grid resolution is uniform throughout the hull, without any need for increased resolution near the interface. Hence, the same grid is applicable to free surface flows at various speeds, where the location of the free surface may vary greatly based on the speed.

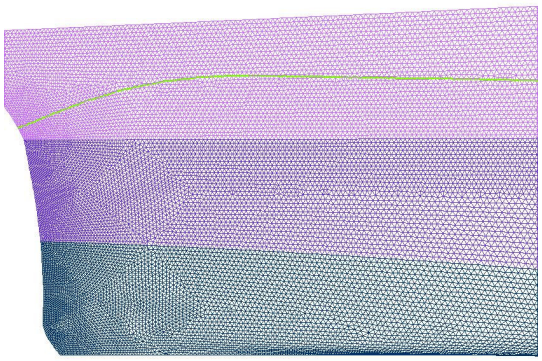

Figure 9. Surface grid resolution near bow of Series 60 along with free surface elevation, shown in green.

C. David Taylor Model Basin (DTMB) Model 5415 Series Hullform.

The DTMB Model 5415 Series hullform is the prototypical naval destroyer hullform, having a large bulbous bow which reduces the elevation of the bow wave peak and a large transom stern, which is the source of the numerical difficulties for free surface simulations. This hullform is strictly a model hull, which has been used in the testing and development of the DDX series naval destroyers, typically at a Froude number of 0.28. At the lower Froude number, the transom is partially wetted and the wetting of the free surface varies with the Reynolds number, making the simulation of the DTMB Model 5415 hullform using a surface tracking approach quite challenging. At the higher Froude number, the bow wave exhibits wave breaking which is not allowed by the surface capturing approach. Excellent examples of this behavior for the similar DDG-51 hullform are shown by DiMascio, et al, using the single-phase level set approach within their structured flow solver[13].

The unstructured grids used to simulate the inviscid flow past the DTMB Model 5415 at a Froude number of 0.28 consisted of a fine grid with 2,132,164 nodes, a medium grid with 1,139,051 nodes, a coarse grid with 624,476 nodes and a very coarse grid with 343,191 nodes, which more closely reflected the expected grid halving. Both sides of the hull were gridded for these simulations. The wave profiles for these four grids are shown in Figure 10. The height of the bow wave increases with grid resolution, but the bow trough and the wave elevations behind the bow wave structure becomes less extreme as the grid is refined, tending towards the experimental results. The rest of wave pattern along the hull smoothes out for the most refined grid, and the drop in the free surface in the stern region is the greatest for the most resolved grid, indicating that the refined grid is capturing the free surface features quite well.

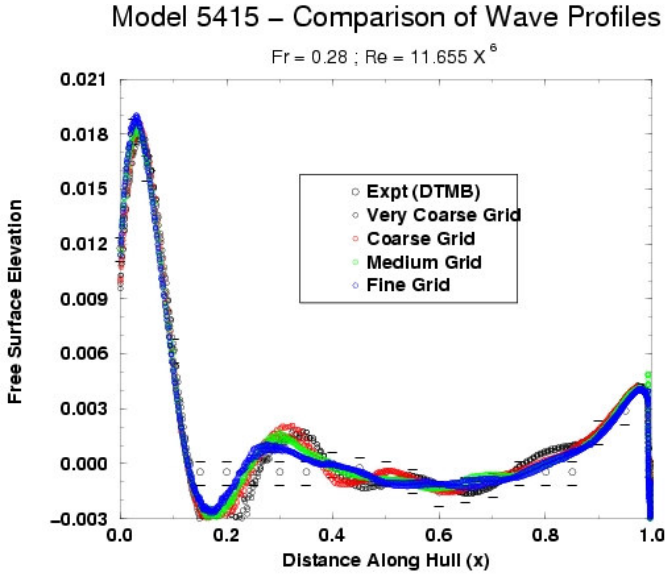

Figure 10. Wave elevations along the hull of DTMB Model 5415.

The free surface elevations away from the hull and in the stern region are shown in Figures 11 and 12, for the most resolved grid. The bow wave pattern, shown in Figure 11, is quite noticeable for approximately one ship length from the bow. The stern wave pattern, presented in Figure 12, can be seen for approximately two ship lengths behind the stern, although the breadth of the waves further downstream are diminished. In the stern region, the stern is in the dry condition, with the free surface detaching from the stern very close to the bottom of the stern, which is consistent with the inviscid (i.e., very high Reynolds number) flow condition. The free surface in the stern region is an inherently unsteady phenomenon, and is sensitive to variations in the grid resolution, resulting in a non-symmetric free surface as is shown in the last image.

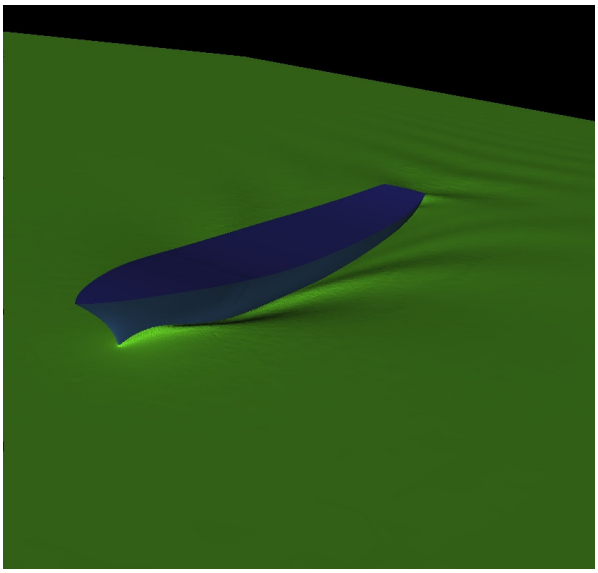

Figure 11. 3D perspective of wave elevations for DTMB Model 5415.

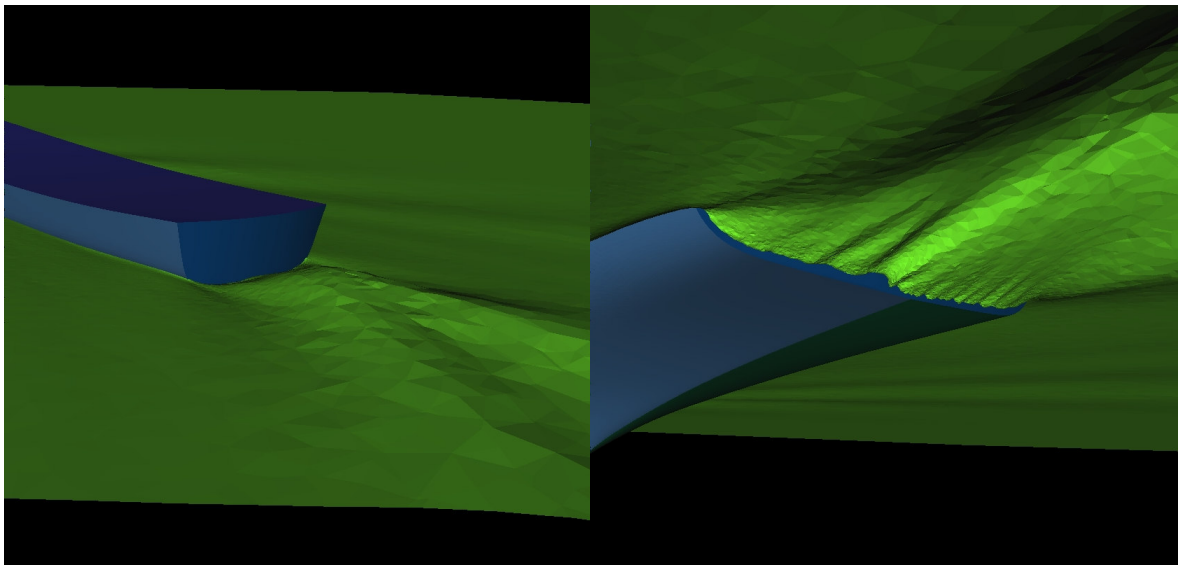

Figure 12. Free surface shape at stern of DTMB Model 5415, as shown from above (left) and below (right). The flow is only slightly attached to the stern of the hull, as is expected for the dry transom condition.

The free surface along the hull and in the stern region is shown in Figures 13 and 14. The bow wave dissipates approximately 40% down the length of the hull due to the loss of grid resolution. However, the free surface in the stern region is well resolved, capturing the physical features well.

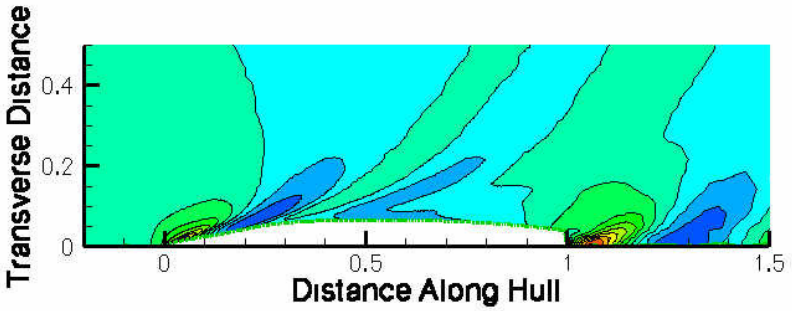

Figure 13. Wave elevations along and behind the DTMB Model 5415 hull.

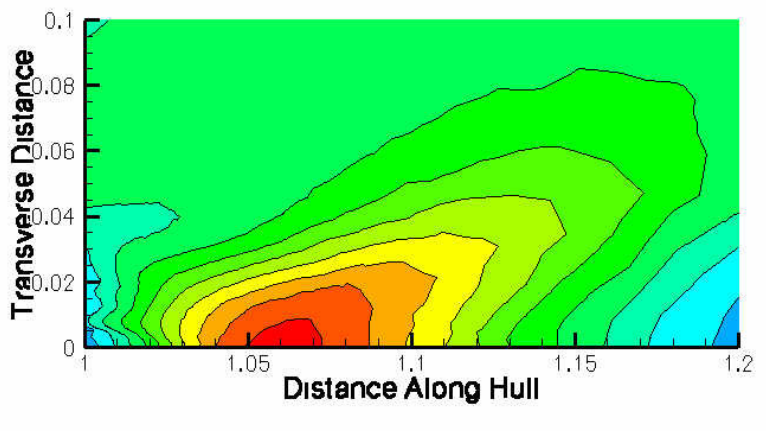

Figure 14. Wave elevations in stern of DTMB Model 5415 hull.

D. America's Cup Yacht

Because of the robustness of the single-phase level set approach, it can be rapidly applied to a wide variety of hullforms, even when the free surface behavior is not known. As an example, the flow past a typical America's Cup yacht was simulated, with no prior knowledge of the wave field. For this simulation, the yacht is sailing directly ahead so that the ship is at a slight angle of attack to the flow, without any tilting of the ship to port or starboard. The stern of the yacht, at rest, extends significantly above the waterline, as does the stern of the Series 60 Cb=0.6 hullform. However, at the Froude number simulated herein, the free surface remains attached to the bottom of the hull until it reaches the stern, which is a transom. This type of behavior would be quite difficult for a surface tracking methodology since the grid would need to stretch a large distance towards the stern.

The images in Figure 15 show the free surface around the America's Cup geometry, showing the rudder and the bulbous counter-weight. Gridding this geometry with an unstructured grid was relatively simple, but would be more complicated with a structured grid. However, the bulbous counter-weight does taper to a sharp trailing edge which is difficult to grid with an unstructured surface mesh.

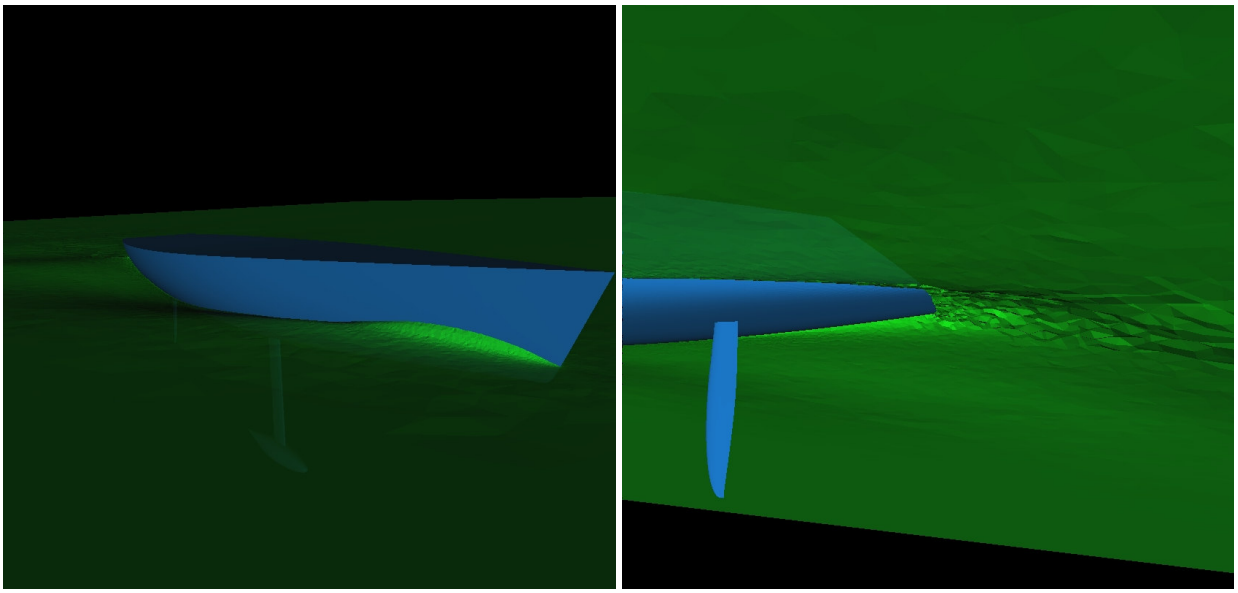

Figure 15. Flow past a typical America's Cup yacht, showing the bow wave (left) and stern effects (right).

E. Notional Water Cannon

As an example of the robustness and wide applicability of this methodology, the flow past a notional water cannon has been simulated. The water cannon consists of a cylinder placed into the water at a 45 degree angle. One end of the cylinder is submerged and envelopes a body-force propulsor, while the other end is above the zero water line. The propulsor forces the water through the cylinder with such force that it shoots out of the end of the cylinder, cleanly detached from the water, arches over and re-enters the water, as is shown in the first image in Figure 16. The flow is also moving from left to right so that it spills over the top of the cylinder, similar to the flow over a partially submerged submarine, which can be seen in the second image in Figure 16. The bottom two images in Figure 16 show the flow complexities in the water jet and in the recirculation behind the water cannon.

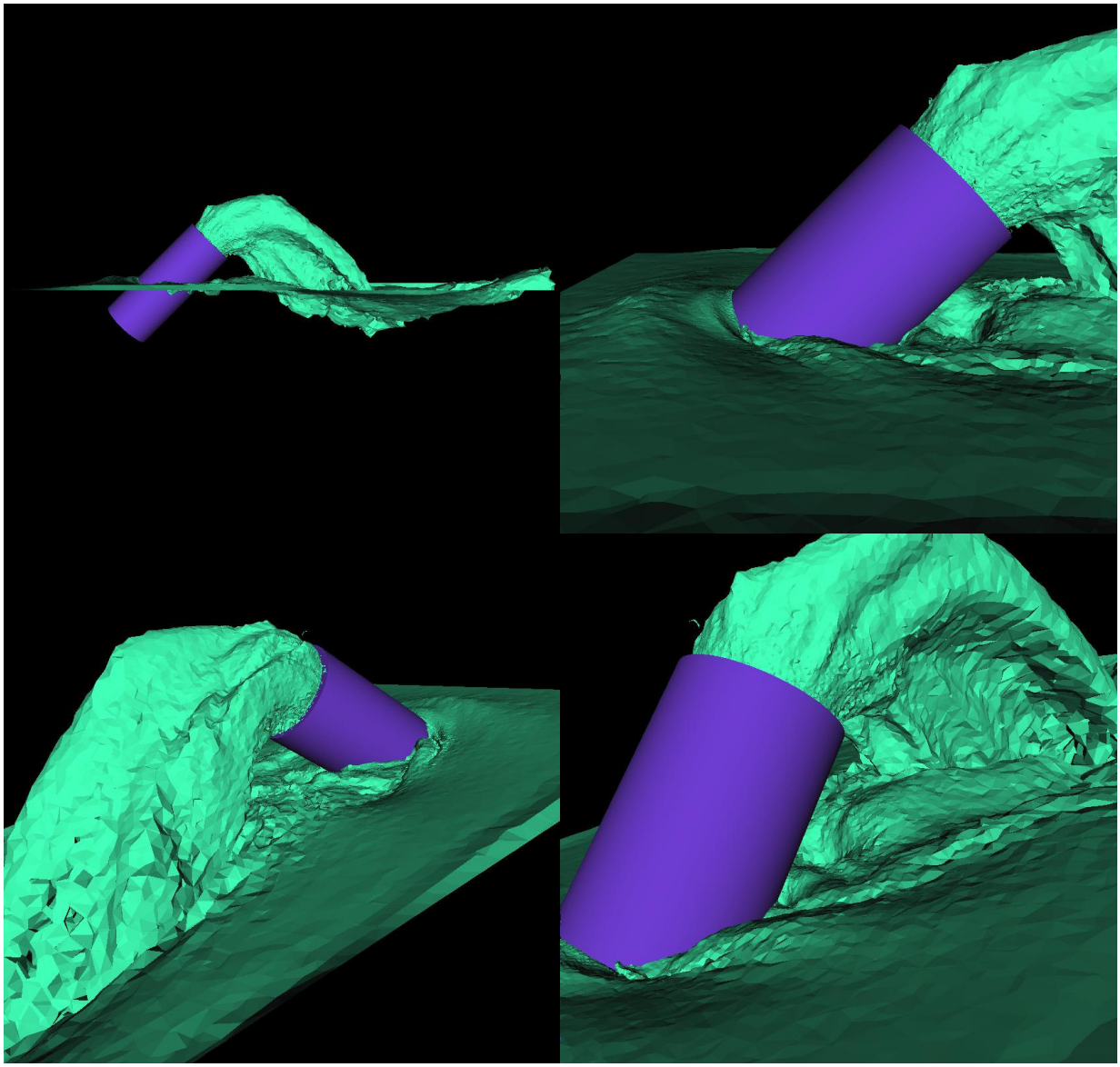

Figure 16. Images of flow erupting from notional water cannon.

IV. Conclusion

The single-phase level set method has been successfully implemented within a modern unstructured flow solver, capable of solving the free surface around complicated hullform and complicated physics, on grids of several million nodes. This single-phase level set method allows for a crisp air/water interface and can simulate cresting, breaking and re-entering waves. The cases shown herein demonstrate that the single-phase level set method simulates the free surface for a variety of hullforms in good agreement with experimental data, as long as the grid resolution is sufficient for maintaining the free surface. The governing equations for the single-phase level set approach are discussed in detail, describing the methods for their discretization using the finite volume method and the appropriate boundary conditions. Several inviscid examples using this methodology have been presented, including flow past the Wigley hull, the Series 60 Cb=0.6 and the naval destroyer DTMB Model 5415 hullform, each of which having a grid refinement study showing the level of grid resolution required by this method. Additionally, this approach was applied to a typical America's Cup yacht geometry, showing its ability to capture the free surface, without the need for prior knowledge of the shape of the free surface. Finally, an example of flow through and out of a notional water cannon was presented, showing that this methodology is applicable to flows where the water shoots upward, arches over and re-enters the main body of water.

This implementation of the single-phase level set methodology generates reasonable agreement with experimental results for several hullforms and demonstrates the required wide applicability and robustness to handle the physical and geometric complexity of free surface flows around naval vessels. In addition, the free surface can be captured precisely within one cell, without smearing the free surface interface, and the wave patterns in the free surface can be maintained downstream of their origination by clustering points in these regions. Future work is needed to validate the methodology for viscous simulations involving highly-stretched anisotropic cells within the boundary layer.

Acknowledgments

The research presented herein was performed by the author while working within the Computational Simulation and Design Center at Mississippi State University and was partially funded through the office of Patrick Purtell at the Office of Naval Research. Additionally, the author would like to thank Len Imas for providing the geometry for the America's Cup hullform.

References

[1]Beddhu, M., Pankajakshan, R., Jiang, M.Y., Remotigue, M., Sheng, C., Taylor, L., Briley, W., and Whitfield, D., "Computation of Nonlinear Turbulent Free Surface Flows Using the Parallel UNCLE Code", *Proceedings of the 23rd Symposium on Naval Hydrodynamics*, Val De Reuil, France, Sept. 2000.

[2]Wilson, R., and Stern, F., "Unsteady RANS Simulation of a Surface Combatant with Roll Motion", *Proceedings of the 24th Symposium on Naval Hydrodynamics*, Fukuoka, Japan, July, 2002.

[3]Weymouth, G. D., Wilson, R. V., and Stern, F., "RANS CFD Prediction of Pitch and Heave Ship Motions in Head Seas", *Proceedings of 8th International Conference on Numerical Ship Hydrodynamics*, Busan, Korea, Sept., 2003.

[4]Li, T., "Effects of Ship Speeds on Viscous Free-Surface Flows around Modern Ships", *Proceedings of the 24th Symposium on Naval Hydrodynamics*, Fukuoka, Japan, July, 2002.

[5]Lin, C., Percival, S., "Free Surface Viscous Flow Computations around a Transom Stern Ship by Chimera Overlapping Scheme", *Proceedings of 23rd Symposium on Naval Hydrodynamics*, Val De Reuil, France, Sept. 2000.

[6]Burg, C. O. E., Sreenivas, K., Hyams, D., and Mitchell, B., "Unstructured Nonlinear Free Surface Flow Solutions: Validation and Verification", AIAA Paper 2002-2977, 32nd AIAA Fluid Dynamics Conference, St. Louis, June, 2002.

[7]Lohner, R.,Yang, C., Onate, E., and Idelssohn, S., "An Unstructured Grid-Based, Parallel Free Surface Solver", AIAA Paper 97-1830.

[8]Hino, T., "An Unstructured Grid Method for Incompressible Viscous Flows With a Free Surface", AIAA Paper 97-0862, Reno, Jan., 1997.

[9]Hirt, C. W., and Nichols, B. D., "Volume of Fluid (VOF) for the Dynamics of Free Boundaries", *Int. J. of Comp. Physics*, 39:201-225, 1981.

[10]Aliabadi, S., Tezduyar, T., "Stabilized-Finite-Element/Interface-Capturing Technique for Parallel Computation of Unsteady Flows with Interfaces", *Computer Methods in Applied Mechanics and Engineering*, 190:243-261, 2000.

[11]CFX Website http://www_waterloo.ansys.com/cfx .

[12]Comet Website http://www.cd-adapco.com .

[13]DiMascio, A., Muscari, R., and Broglia, R., "Computation of Free Surface Flows Around Ship Hulls by a Level-Set Approach", *Proceedings of 8th Int. Conf. on Num. Ship Hydrodynamics*, Busan, Korea, Sept. 2003.

[14]Chorin, A. J., "A Numerical Method for Solving Incompressible Viscous Flow Problems," *J. Comput. Phys.*, Vol. 2, No. 1, August 1967, pp. 12-26.
[15]Pan, D., Chakravarthy, S., "Unified Formulation for Incompressible Flows," AIAA Paper 89-0122, *Proceeding of 27th AIAA Aerospace Sciences Meeting*, Reno, NV, Jan. 1989.
[16]Rogers, S. E., and Kwak, D., "Upwind Differencing for the Time-Accurate Incompressible Navier-Stokes Equations," *AIAA J.*, Vol. 28, No. 2, 1990, pp. 253–262.
[17]Taylor, L. K., "Unsteady Three-Dimensional Incompressible Algorithm Based on Artificial Compressibility," Ph.D. dissertation, Mississippi State University, May 1991.
[18]Spalart, P. R., and Allmaras, S. R., "A One-Equation Turbulence Model for Aerodynamic Flows", AIAA Paper 92-0439, *Proceedings of 30th AIAA Aerospace Sciences Meeting*, Reno, NV, Jan., 1992.
[19]Roe, P. L., "Approximate Riemann Solvers, Parameter Vector, and Difference Schemes," *Journal of Computational Physics*, Vol. 43, Number 2, October 1981, pp. 357–372.
[20]Burg, C. O. E., Sreenivas, K., Hyams, D., and Mitchell, B., "Unstructured Nonlinear Free Surface Simulations for the Fully-Appended DTMB Model 5415 Series Hull Including Rotating Propulsors", *Proceedings of 24th Symposium on Naval Hydrodynamics*, Fukuoka, Japan, July, 2002.
[21]Blades, E., Marcum, D., and Mitchell, B., "Simulation of Spinning Missile Flow Fields Using U2NCLE", AIAA Paper 2002-2797, *Proceedings of 32nd AIAA Fluid Dynamics Conf.*, St. Louis, June, 2002.
[22]Sreenivas, K., Hyams, D., Mitchell, B., Taylor, L., Marcum, D., and Whitfield, D., "Computation of Vortex-Intensive Incompressible Flow Fields", AIAA Paper 2002-3306, *Proceedings of 32nd AIAA Fluid Dynamics Conf.*, St. Louis, June, 2002.
[23]Hyams, D. G., "An Investigation of Parallel Implicit Solution Algorithms for Incompressible Flows on Unstructured Topologies", Ph.D. Thesis, May 2001, Mississippi State University, http://library.msstate.edu/etd .
[24]Hyams, D. G., Sreenivas, K., Sheng, C., Briley, W. R., Marcum, D. L., and Whitfield, D. L., "An Investigation of Parallel Implicit Solution Algorithms for Incompressible Flows on Multielement Unstructured Topologies", AIAA Paper 2000-0271, *Proceedings of 39th AIAA Aerospace Sciences Meeting*, Reno, Jan., 2000.
[25]Marcum, D. L., Weatherhill, N. P., Marchant, M. J., and Beaven, F., "Generation of Unstructured Grids for Viscous Flow Applications," AIAA Paper 95-0212, *Proceeding of 33rd Aerospace Science Meeting and Exhibit*, Reno, NV, January, 1995.
[26]Marcum, D. L., and Weatherhill, N. P., "Unstructured Grid Generation Using Iterative Point Insertion and Local Reconnection," *AIAA J.*, Vol. 33, No. 9, September 1995, pp. 1619-1625.
[27]Burg, C. O. E., "Higher Order Variable Extrapolation for Unstructured Finite Volume RANS Flow Solvers", AIAA Paper 2005-4999, *Proceedings of 17th AIAA Computational Fluid Dynamics Conference*, Ontario, Canada, June, 2005.
[2\8]Whitfield, D. L., *Newton-Relaxation Schemes for Nonlinear Hyperbolic Systems*, Engineering and Industrial Research Station Report MSSU-EIRS-ASE-90-3, Mississippi State University, Miss., October 1990.
[29]Whitfield, D. L. and Taylor, L. K., "Discretized Newton-Relaxation Solution of High Resolution Flux-Difference Split Schemes," AIAA Paper 91-1539, *Proceedings of AIAA 10th Computational Fluid Dynamics Conference, June*, 1991.
[30]*Cooperative Experiments on Wigley Parabolic Models in Japan*, Nineteenth R. C. Report, International Towing Tank Conference (ITTC), 1983.